https://doi.org/10.48048/tis.2023.4600

Analysis and Simulation of Mathematical Model of COVID-19 Incorporated with Vaccination and Media Induced Fear

Kehinde Adekunle Bashiru[1,*], Mutairu Kayode Kolawole[2] and Mutiu Lawal Olaosebikan[2]

[1]Department of Statistics, Faculty of Basic and Applied Sciences, Osun State University, Osogbo, Nigeria
[2]Department of Mathematical Sciences, Faculty of Basic and Applied Sciences, Osun state University, Osogbo, Nigeria

([*]Corresponding author's e-mail: kehindebashiru@uniosun.edu.ng)

Received: 9 June 2022, Revised: 21 July 2022, Accepted: 28 July 2022, Published: 23 January 2023

Abstract

COVID-19 pandemic is now increasing concern to authorities and public health officials. The study is aimed to investigate the impact of vaccination in the absence of media induced fear. In this research, analysis and simulation of a mathematical model of COVID-19 incorporated with media induced fear and vaccination was made, the total population is divided into 5 sub-population classes; Susceptible, Exposed, Infected, Quarantine and Recovery. The disease free and the endemic equilibrium of the model were carried out and the basic reproduction number was obtained using the next generation matrix. The stability analysis of the model was done and it was ascertained that the disease free equilibrium of the biological model is stable. Due to its efficiency and accuracy in handling nonlinear coupled ordinary differential equations, the homotopy perturbation method is applied to obtain the approximate solution of the mathematical model and the obtained results was simulated using the computation software Maple 18 to study the impact of vaccination in each compartment of the model when the media induced fear. The outcome of the simulation process were presented graphically and interpreted accordingly and it was discovered that in eradicating the spread of COVID-19 in a society where there is no fear, vaccination is an alternative and better measure.

Keywords: COVID-19, Vaccination, Disease free equilibrium, Endemic equilibrium, Homotopy, Perturbation method

Introduction

Mathematical modeling has been regarded as an optimal control measure to curb the spread of infectious diseases such as COVID-19. Authors such as [1] conducted a research on mathematical model for an effective management of HIV infection. [2] Researched on the numerical simulation of SEIRS epidemic model with saturated incidence rate considering the saturation term for susceptible individuals. In their research, they establish the disease free and endemic equilibrium points derive the basic reproduction number using the next generation matrix, establish the local stability, global stability of both the disease free and endemic equilibrium respectively. Furthering in the area of disease control strategy, computer simulations are often applied by researchers after obtaining the approximate solutions of these mathematical models. Several methods such as the one introduced by [3,4] has been used by researchers such [5-7], to conduct investigations on different mathematical models.[8,9], applied a numerical method introduced by [10], to carry out simulation in their model. It is no news that COVID-19 pandemic has been a major threat to the existing population of the globe since it outbreaks in Wuhan China (2019), [11-19]. Disease prevention is influenced by media coverage, since the spread of communicable diseases is subject to the information and spreading potentials of the diseases [15].

In this research a control strategy on the curb of the virus based on vaccination is studied. A 5 compartmental time-based epidemic model of COVID-19 virus adopted from [11] is modified by incorporating vaccination parameter ρ into the susceptible and recovered class to examine the effect of vaccination rate.

Materials and methods

Model equations

The total population is divided into 5 sub-population classes; (S) Susceptible, (E) Exposed, (I) Infected, (Q) Quarantine and (R) Recovery.

$$\frac{dS}{dt} = r - \frac{\beta SI}{I + \alpha I} - \rho S - \mu S \tag{1}$$

$$\frac{dE}{dt} = \frac{\beta SI}{I + \alpha I} - (c + \mu)E \tag{2}$$

$$\frac{dI}{dt} = CE - (\gamma + d + d_l + \mu)I \tag{3}$$

$$\frac{dQ}{dt} = \gamma I - (\lambda + \mu)Q \tag{4}$$

$$\frac{dR}{dt} = d_l I + \lambda Q - \mu R + \rho S \tag{5}$$

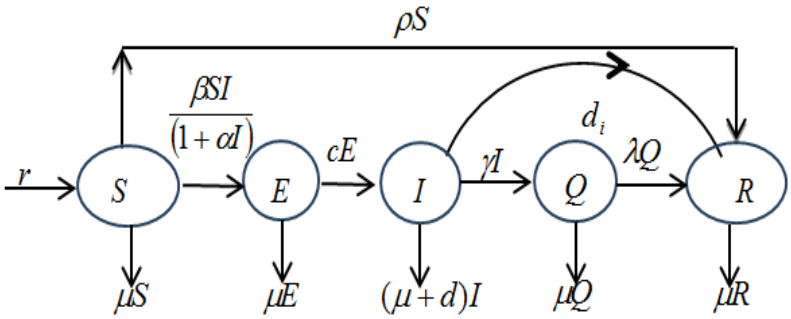

Proposed Schematic Diagram for the transmission of COVID-19

Equilibrium state

At equilibrium state;

$$\frac{dS}{dt} = \frac{dE}{dt} = \frac{dI}{dt} = \frac{dQ}{dt} = \frac{dR}{dt} = 0$$

such that Eqs. (1) - (5) gives;

$$0 = r - \frac{\beta SI}{I + \alpha I} - \rho S - \mu S \tag{6}$$

$$0 = \frac{\beta SI}{I + \alpha I} - (c + \mu)E \tag{7}$$

$$0 = CE - (\gamma + d + d_l + \mu)I \tag{8}$$

$$0 = \gamma I - (\lambda + \mu)Q \tag{9}$$

$$0 = d_l I + \lambda Q - \mu R + \rho S \tag{10}$$

Disease-free equilibrium

The fixed state of the system (6) - (10) above satisfies the disease-free equilibrium (at Disease Free State) E = I = 0. Solving the system Eq. (6) - (10) simultaneously, thus obtained (11) as disease free equilibrium;

$$(S, E, I, Q, R) = (\frac{r}{\rho + \mu}, 0, 0, 0, \frac{\rho r}{\mu(\rho + \mu)}) \tag{11}$$

Basic reproduction number

The infected compartments of the epidemic model are $E(t), I(t)\ and\ Q(t)$. Extracting the compartments off the model;

$$\frac{dE}{dt} = \frac{\beta SI}{I + \alpha I} - (c + \mu)E \tag{12}$$

$$\frac{dI}{dt} = CE - (\gamma + d + d_l + \mu)I \tag{13}$$

$$\frac{dQ}{dt} = \gamma I - (\lambda + \mu)Q \tag{14}$$

The next generation matrix is applied to obtain the basic reproduction number.

Thus, $G = FV^{-1}$ (15)

The secondary infection;

$$F^{'} = \begin{bmatrix} \frac{\beta SI}{I + \alpha I} \\ 0 \\ 0 \end{bmatrix} \tag{16}$$

and;

$$V^{'} = \begin{bmatrix} -(c + \mu)E \\ CE - (\gamma + d + d_l + \mu)I \\ \gamma I - (\lambda + \mu)Q \end{bmatrix} \tag{17}$$

$$F = J(F^{'})\ \ and\ \ V = J(V^{'})$$

$$F' = \begin{bmatrix} 0 & \frac{\beta S}{(I+\alpha I)^2} & 0 \\ 0 & 0 & 0 \\ 0 & 0 & 0 \end{bmatrix} \quad and \quad V \begin{bmatrix} (c+\mu) & 0 & 0 \\ -c & (\gamma + d + d_l + \mu) & 0 \\ 0 & -\gamma & (\lambda + \mu) \end{bmatrix} \tag{18}$$

computing for V^{-1},

$$V^{-1} = \begin{bmatrix} \frac{1}{c+\mu} & 0 & 0 \\ \frac{c}{(\gamma + d + d_l + \mu)(c+\mu)} & \frac{1}{(\gamma + d + d_l + \mu)} & 0 \\ \frac{c\gamma}{(\gamma + d + d_l + \mu)(c+\mu)} & \frac{\gamma}{(\gamma + d + d_l + \mu)(\lambda + \mu)} & \frac{1}{(\lambda + \mu)} \end{bmatrix} \tag{19}$$

since $G = FV^{-1}$, therefore;

$$G = \begin{bmatrix} \frac{-\beta Sc}{(\gamma + d + d_l + \mu)(c+\mu)(1+\alpha I)^2} & \frac{-\beta S}{(\gamma + d + d_l + \mu)(1+\alpha I)^2} & 0 \\ 0 & 0 & 0 \\ 0 & 0 & 0 \end{bmatrix} \tag{20}$$

computing for the Eigenvalues of G, $|G - \lambda I| = 0$ therefore;

$$\lambda = 0,0, \frac{-\beta Sc}{(\gamma + d + d_l + \mu)(c+\mu)(1+\alpha I)^2} \tag{21}$$

The spectral radius of the matrix G is the largest Eigenvalue, therefore;

$$R_0 = \frac{-\beta Sc}{(\gamma + d + d_l + \mu)(c+\mu)(1+\alpha I)^2} \tag{22}$$

Endemic equilibrium

In this section, the endemic equilibrium of the model is obtained by solving the system of Eqs. (1) - (5) concurrently when;

$$\frac{dS}{dt} = \frac{dE}{dt} = \frac{dI}{dt} = \frac{dQ}{dt} = \frac{dR}{dt} \neq 0.$$

for brevity, the following parameters are denoted;

$$(\lambda + \mu) = d_1, \quad (\gamma + d + d_l + \mu) = d_2 \quad (c+\mu) = d_3 \quad (\rho + \mu) = d_4 \quad (\beta + \rho\alpha + \mu\alpha) = d_5$$

and the endemic equilibrium of the model is given as;

$$S^* = \frac{S(d_5 - \alpha d_4) + \alpha r R_0 (1+\alpha I)^2}{R_0 (1+\alpha I)^2}$$

$$E^* = \frac{d_2 [r R_0 (1+\alpha I)^2 - S d_4]}{S c d_5}$$

$$I^* = \frac{[r R_0 (1+\alpha I)^2 - s d_4]}{S c d_5}$$

$$E^* = \frac{\gamma [r R_0 (1+\alpha I)^2 - S d_4]}{S d_1 d_5}$$

$$E^* = \frac{d_l I^* + \lambda Q^* + \rho S^*}{\mu}$$

Stability analysis

The local stability of the disease-free equilibrium is carried out in this section. The Jacobian of the system of Eqs. (1) - (5) is constructed and evaluated at the disease-free equilibrium;

$$(\frac{r}{\rho+\mu}, 0, 0, 0, \frac{\rho r}{\mu(\rho+\mu)})$$

$$J = \begin{bmatrix} \frac{-\beta}{(1+\alpha I)} - (\rho+\mu) & 0 & \frac{-\beta S}{(1+\alpha I)^2} & 0 & 0 \\ \frac{\beta I}{(1+\alpha I)} & -(c+\mu) & \frac{\beta S}{(1+\alpha I)^2} & 0 & 0 \\ 0 & c & (\gamma + d + d_l + \mu) & 0 & 0 \\ 0 & 0 & \gamma & -(\lambda+\mu) & 0 \\ 0 & 0 & d_l & \lambda & -\mu \end{bmatrix} \quad (23)$$

evaluating J at disease free equilibrium;

$$J = \begin{bmatrix} -(\rho+\mu) & 0 & \frac{-\beta S}{(\rho+\mu)} & 0 & 0 \\ 0 & -(c+\mu) & \frac{\beta S}{(\rho+\mu)} & 0 & 0 \\ 0 & c & -(\gamma + d + d_l + \mu) & 0 & 0 \\ 0 & 0 & \gamma & -(\lambda+\mu) & 0 \\ 0 & 0 & d_l & \lambda & -\mu \end{bmatrix} \quad (24)$$

applying previously defined notations;

$$J=\begin{bmatrix} -d_4 & 0 & -d_4 & 0 & 0 \\ 0 & -d_3 & d_6 & 0 & 0 \\ 0 & c & -d_2 & 0 & 0 \\ 0 & 0 & \gamma & -(\lambda+\mu) & 0 \\ \rho & 0 & d_1 & \lambda & -\mu \end{bmatrix} \tag{25}$$

The Eigen values of J is calculated, so that if $|J-\lambda I|=0$;

$$\lambda_1=-(\lambda+\mu)\ \ \lambda_2=-(\rho+\mu)\ \ \lambda_3=-\mu$$

$$\lambda_4=-\frac{1}{2}\left[d_2+d_3-\sqrt{(d_2-d_3)^2+4cd_6}\right]$$

$$\lambda_5=-\frac{1}{2}\left[d_2+d_3+\sqrt{(d_2-d_3)^2+4cd_6}\right]$$

It is obvious that $\lambda_1\,\lambda_2\,\lambda_3<0.$ Therefore, $\lambda_4\ and\ \lambda_5$ must be real and negative for the disease-free equilibrium to be stable.

Therefore $d_6>0$ for $\lambda_{\backslash 4}\ and\ \lambda_{\backslash 5}$ to be real and If so, $\lambda_{\backslash 5}<0$. Also, if $d_2+d_3>0$ then $\lambda_{\backslash 4}<0$ and the equilibrium is locally stable. Otherwise, it is unstable.

Numerical solution and simulation

Homotopy perturbation method

Here, the approximate solution of the model will be obtain to conduct the simulation process of the impact of vaccination rate in the model, the homotopy perturbation method is employed to solve the coupled differential equation. The basic idea of homotopy perturbation method presented by [3] is illustrated by considering a non-linear differential equation of the form;

$$A(x)-B(z)=0\,,z\in\xi \tag{26}$$

subject to the boundary condition;

$$\Gamma(x,\frac{\partial x}{d\eta})=0 \tag{27}$$

The function $A(x)$ can be expressed as $L_T(x)+N_T(x)$ where $L_T(x)$ represent the linear terms and $N_T(x)$ represent the non-linear terms such that Eq. (26) becomes;

$$L_T(x)+N_T(x)-B(z)=0\ z\in\xi \tag{28}$$

according to He [3], an homotopy can be constructed for (28) such that;

$$H(y,p)=(1-p)[L(y)-L(x_0)]+p[A(y)-B(z)]=0 \tag{29}$$

where, $y(z,p):=\xi\times[0,1]\to R$

Thus, at p = 0,

$$H(y,0) = L(y) - L(x_0) = 0 \tag{30}$$

and at p = 1 the following equation is obtained as follows;

$$H(y,1) = A(y) - B(z) = 0 \ \forall \quad p \in [0,1].$$

The approximate solution to the problem is figured as a power series embedding a parameter p expressible as;

$$y(x) = y_0(x) + py_1(x) + p^2 y_2(x) + \cdots + p^n y_n.$$

so that the best approximate solution is obtained for (26) when;

$$\lim_{p \to 1} y = y_0 + y_1 + y_2 + \ldots y_n \tag{31}$$

Application of the homotopy perturbation method

In this section, the approximate analytical method illustrated from Eqs. (26) - (31) is extended to obtain the solution of (6) - (10). To begin with, the series solution of the system of Eq. (6) - (10) is assumed to be;

$$\begin{aligned}
y(t) &= y_0(t) + py_1(t) + p^2 y_2(t) + \cdots + p^n y_n \\
S(t) &= s_0(t) + ps_1(t) + p^2 s_2(t) + \ldots + p^n s_n(t) \\
E(t) &= e_0(t) + pe_1(t) + p^2 e_2(t) + \ldots p^n e_n(t) \\
I(t) &= i_0(t) + pi_1(t) + p^2 i_2(t) + \ldots + p^n i_n(t) \\
Q(t) &= q_0(t) + pq_1(t) + p^2 q_2(t) + \ldots + p^n q_n(t) \\
R(t) &= r_0(t) + pr_1(t) + p^2 r_2(t) + \ldots + p^n r_n(t)
\end{aligned} \tag{32}$$

next is constructing a homotopy for the system such that;

$$\begin{aligned}
(1-p)\left\{\frac{dS}{dt}\right\} &= p\left\{\frac{dS}{dt} - r + \beta SI\delta + \mu S + \rho S\right\} \\
(1-p)\left\{\frac{dE}{dt}\right\} &= p\left\{\frac{dE}{dt} - \beta SI\delta + (\mu + c)E\right\} \\
(1-p)\left\{\frac{dI}{dt}\right\} &= p\left\{\frac{dI}{dt} - CE + (\gamma + \delta + \mu + d_l)I\right\} \\
(1-p)\left\{\frac{dQ}{dt}\right\} &= p\left\{\frac{dQ}{dt} - \gamma I + (\lambda + \mu)Q\right\} \\
(1-p)\left\{\frac{dR}{dt}\right\} &= p\left\{\frac{dR}{dt} - d_l I - \lambda Q + \mu R - \rho S\right\}
\end{aligned} \tag{33}$$

where $\delta = \dfrac{1}{1+\alpha I}$. In the absence of fear, $\alpha = 0$ and there is no reduction in the disease transmission rate. The assumed series solutions in (22) were substituted appropriately into their respective functions in (23), and equal powers of p are compared to obtain;

$$p^0 \ \frac{ds_0}{dt} = 0, \frac{de_0}{dt} = 0, \frac{di_0}{dt} = 0, \frac{dq_0}{dt} = 0, \frac{dr_0}{dt} = 0 \tag{34}$$

Eq. (34) is solved and the following solutions are obtained as initial approximations.

$$s_0(t) = s_0,\ e_0(t) = e_0,\ i_0(t) = i_0,\ q_0(t) = q_0,\ r_0(t) = r_0$$

also equating like powers of p^1;

$$\begin{aligned}
&\frac{ds_1(t)}{dt} - r - \mu s_0(t) + \beta\delta i_0(t)s_0(t) + \rho s_0(t) = 0\\
&\frac{de_1(t)}{dt} + ce_0(t) - \beta\delta i_0(t)s_0(t) + \mu e_0(t) = 0\\
&\frac{di_1(t)}{dt} + \mu i_0(t) - ce_0(t) + d_l i_0(t) + di_0(t) + \gamma i_0(t) = 0\\
&\frac{dq_1(t)}{dt} + \lambda q_0(t) - \gamma i_0(t) + \mu q_0(t) = 0\\
&\frac{dr_1(t)}{dt} - \lambda q_0(t) - d_l i_0(t) - \rho s_0(t) + \mu r_0(t) = 0
\end{aligned} \tag{35}$$

and similarly solving the system of equations above, the 1st approximate solutions presented in Eq. (36);

$$\begin{aligned}
s_1(t) &= (-\rho s_0 + r - \beta\delta i_0 s_0 - \mu s_0)t\\
e_1(t) &= (-ce_0 + \beta\delta i_0 s_0 - \mu e_0)t\\
i_1(t) &= (-\mu i_0 + ce_0 + \beta\delta s_0 - \mu e_0)t\\
q_1(t) &= (-\lambda q_0 + \gamma i_0 - \mu q_0)t\\
r_1(t) &= (\lambda q_0 + d_l i_0 + \rho s_0 - \mu r_0)t
\end{aligned} \tag{36}$$

The like powers of p^2 as well yield the following equations;

$$\begin{aligned}
&\frac{ds_2(t)}{dt} - r - \mu s_1(t) + \beta\delta i_1(t)s_1(t) + \rho s_1(t) = 0\\
&\frac{de_2(t)}{dt} + ce_1(t) - \beta\delta i_1(t)s_1(t) + \mu e_1(t) = 0\\
&\frac{di_2(t)}{dt} + \mu i_1(t) - ce_1(t) + d_l i_1(t) + di_1(t) + \gamma i_1(t) = 0\\
&\frac{dq_2(t)}{dt} + \lambda q_1(t) - \gamma i_1(t) + \mu q_1(t) = 0\\
&\frac{dr_2(t)}{dt} - \lambda q_1(t) - d_l i_1(t) - \rho s_1(t) + \mu r_1(t) = 0
\end{aligned} \tag{37}$$

such that the solution to the system of Eq. (35) as well yields;

$$
\begin{aligned}
s_2(t) &= \left\{ \begin{array}{l} \frac{t^2}{2}(\mu^2 s_0 + 2\mu\rho s_0 + 3\mu\beta\delta s_0 i_0 - r\mu + 2\beta\delta i_0 \rho s_0 + \beta^2\delta^2 + {i_0}^2 s_0 \\ -\beta\delta i_0 r + \rho^2 s_0 - r\rho + \beta\delta s_0 \gamma i_0 + \beta\delta s_0 d i_0 - \beta\delta s_0 c e_0 + \beta\delta s_0 d_l i_0) \end{array} \right\} \\
e_2(t) &= \left\{ \begin{array}{l} -\frac{t^2}{2}(3\mu\beta\delta\rho s_0 i_0 + \beta\delta r s_0 i_0 \rho - \beta^2\delta^2 i^2 s_0 - \beta\delta i_0 r + c\beta\delta s_0 i_0 - 2e_0\mu c \\ -e_0 c^2 + \beta\delta s_0 i_0 \gamma + \beta\delta s_0 i_0 d - \beta\delta s_0 c e_0 + \beta\delta s_0 i_0 d_l - e_0\mu^2) \end{array} \right\} \\
i_2(t) &= \left\{ \begin{array}{l} \frac{t^2}{2}(2\gamma\mu i_0 - \gamma c e_0 + 2\gamma d_l i_0 + 2\gamma d i_0 + \gamma^2 i_0 - e_0 c^2 + c\beta\delta s_0 i_0 - 2e_0\mu c + 2d_l\mu i_0 \\ -2e_0\mu c + 2d_l\mu i_0 - d_l c e_0 + {d_l}^2 i_0 + 2d_l d i_0 + 2d\mu i_0 - d c e_0 + d^2 i_0 + \mu^2 i_0) \end{array} \right\} \\
q_2(t) &= \left\{ -\frac{t^2}{2}(\gamma c e_0 - \gamma d_l i_0 - \gamma d i_0 - \gamma^2 i_0 - q_0\lambda^2 + \gamma\lambda i_0 - 2q_0\mu\lambda - q_0\mu^2) \right\} \\
r_2(t) &= \left\{ \begin{array}{l} \frac{t^2}{2}(-q\lambda^2 + \gamma i_0 - 2q_0\mu\lambda - 2d_l\mu i_0 + d_l c e_0 - {d_l}^2 i_0 - d_l d i_0 \\ -\gamma d_l i_0 - 2s_0\rho^2 + r\rho - \beta\delta\rho s_0 i_0 - 2i_0 s_0\rho\mu + r_0\mu^2) \end{array} \right\}
\end{aligned} \tag{38}
$$

With the aid of computation software Maple 18, the process is repeated up to the 4th iteration and the approximate solutions of each of the compartments is represented as;

$$
\begin{aligned}
S(t) &= s_0(t) + s_1(t) + s_2(t) + s_3(t) + s_4(t) \ldots + s_n(t) \\
E(t) &= e_0(t) + e_1(t) + e_2(t) + e_3(t) + e_4(t) \ldots + e_n(t) \\
I(t) &= i_0(t) + i_1(t) + i_2(t) + i_3(t) + i_4(t) \ldots + i_n(t) \\
Q(t) &= q_0(t) + q_1(t) + q_2(t) + q_3(t) + q_4(t) \ldots + q_n(t) \\
R(t) &= r_0(t) + r_1(t) + r_2(t) + r_3(t) + r_4(t) \ldots + r_n(t)
\end{aligned} \tag{39}
$$

Such that evaluation of the obtained results using the following values for their respective parameters, the obtained series solutions are obtained as;

Table 1 Parameters, description, values and reference.

Parameter	Description	Value	Reference
c	Infection rate from exposed	0.1818	[12]
d	Disease-induced death	0.0097	[13]
μ	Natural death rate	0.001	[14]
R	Recruitment rate	0.0005812	[14]
β	Disease transmission rate	0.05	Estimated
α	Effect of fear through media	$0 \le \alpha \le 1$	[15]
δ	Fear factor	1	Estimated
γ	Isolation Rate of infected people.	0.0802	[14]
λ	Recuperation rate from isolated	0.000487	[13]
d_1	Recovery rate of infected individual	0.027	[14]
s_0	Initial susceptible population	30	Assumed

Parameter	Description	Value	Reference
e_0	Initial exposed population	22	Assumed
i_0	Initial infected population	10	Assumed
q_0	Initial isolated population	17	Assumed
r_0	Initial recovered population	15	Assumed

$$S(t)=\left\{\begin{array}{l}30+(-15.029418\,8-30\rho)t+(3.298838819+30.0594188\,\rho+30\rho^2)\frac{t^2}{2}\\-(30\rho^3+9.896807640\rho+45.0894188\,\rho^2-0.09149304\,758)\frac{t^3}{6}\\(60.119418\,8\rho^3+3.724427793\rho+19.79390646\rho^2+30\rho^4+4.045198182)\frac{t^4}{24}\end{array}\right\}$$

$$E(t)=\left\{\begin{array}{l}22+10.9784t+(5.290660920+15\rho)\frac{t^2}{2}-(30\rho^3+9.309909400\rho+15\rho^2\\-0.87234092\,85)\frac{t^3}{6}-(15\rho^3+5.507875466\rho+12.594009400\rho^2+4.204753608)\frac{t^4}{24}\end{array}\right\}$$

$$I(t)=\left\{\begin{array}{l}10+2.820600000t+(0.831662190\,0)t^2-(2.727000\rho-1.157948100)\frac{t^3}{6}\\-(2.014054829\rho+2.727000\rho^2+0.295113659\,7)\frac{t^4}{24}\end{array}\right\}$$

$$Q(t)=\left\{\begin{array}{l}17+0.776721000\,0t+0.112528568\,0t^2-0.022177325\,90t^3\\-(0.218705400\,0\rho+0.093065303\,74)\frac{t^4}{24}\end{array}\right\}$$

$$R(t)=\left\{\begin{array}{l}15+(30\rho+0.263279000\,0)t+(0.076271184\,13+15.0594188\,\rho-30\rho^2)\frac{t^2}{2}\\-(-30\rho^3+3.313898238\rho+30.0894188\,\rho^2-0.044943089\,91)\frac{t^3}{6}+(-0.031244\,73963\\+0.014550150\,39\rho-9.926897060\rho^2-45.1194188\,\rho^3-30\rho^4)\frac{t^4}{24}\end{array}\right\}$$

Results and discussion

In this section the outcome of computer simulation process carried out using the computation software Maple 18 are presented. The influence of the incorporated vaccination parameter ρ is examined on the susceptible, exposed and recovered class on the interval $0 \le \rho < 1$. The Graphs are discussed accordingly to give a clear interpretation of the influence of vaccination rate in the model.

In this section the outcome of computer simulation process carried out using the computation software Maple 18 are presented. The influence of the incorporated vaccination parameter ρ is examined on the susceptible, exposed and recovered class on the interval $0 \le \rho < 1$. The Graphs are discussed accordingly to give a clear interpretation of the influence of vaccination rate in the model.

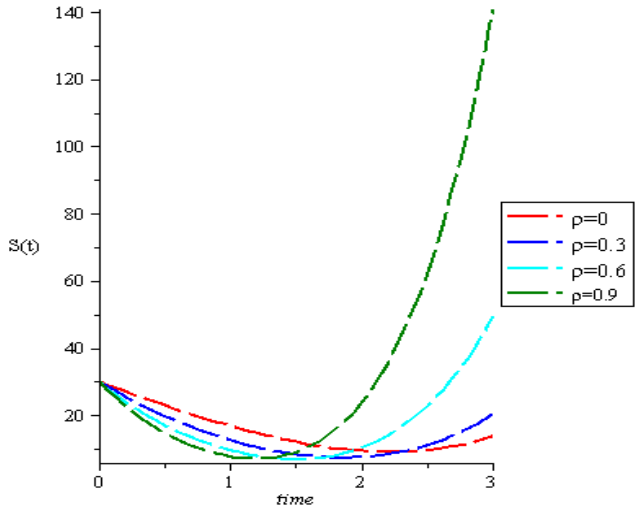

Figure 1 Showing the influence of vaccination rate on the susceptible class.

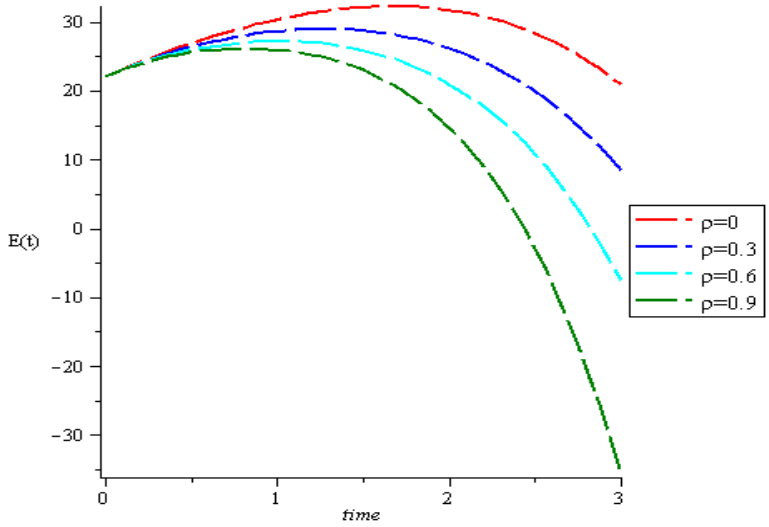

Figure 2 Showing the influence of vaccination rate on the exposed class.

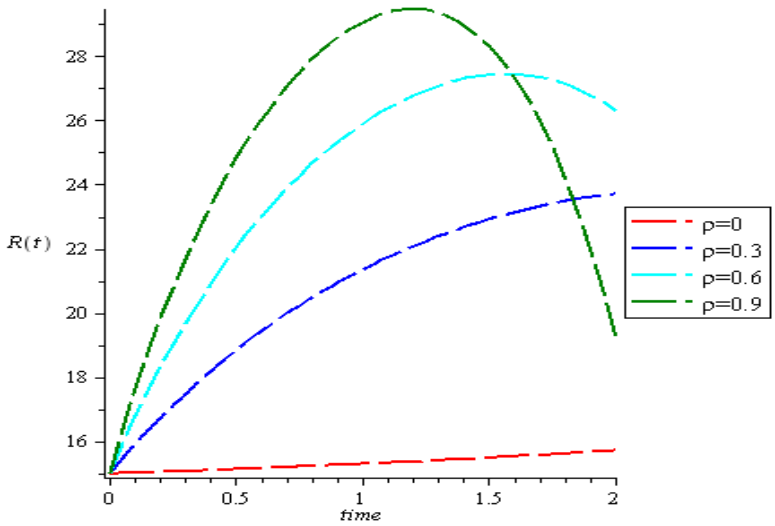

Figure 3 Showing the influence of vaccination rate on the recovered class.

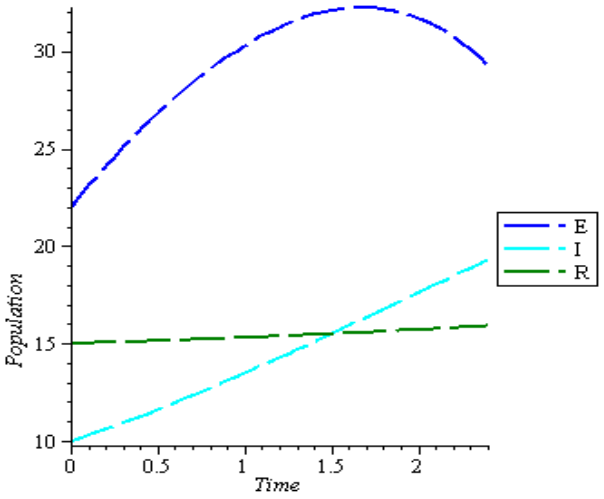

Figure 4 Influence of vaccination rate on the E_I_R at $\rho = 0$.

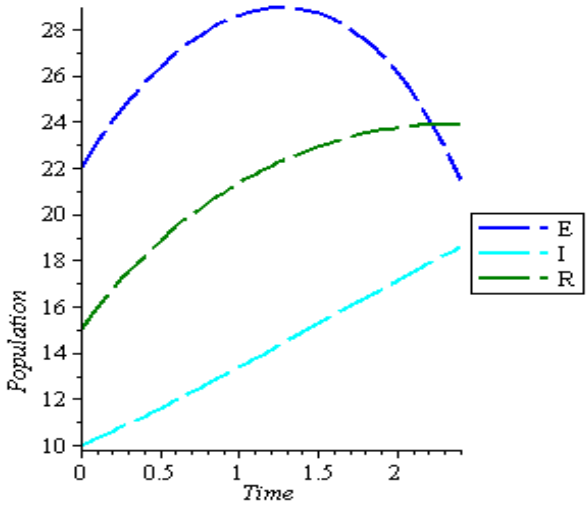

Figure 5 Influence of vaccination rate on the E_I_R at $\rho = 0.3$.

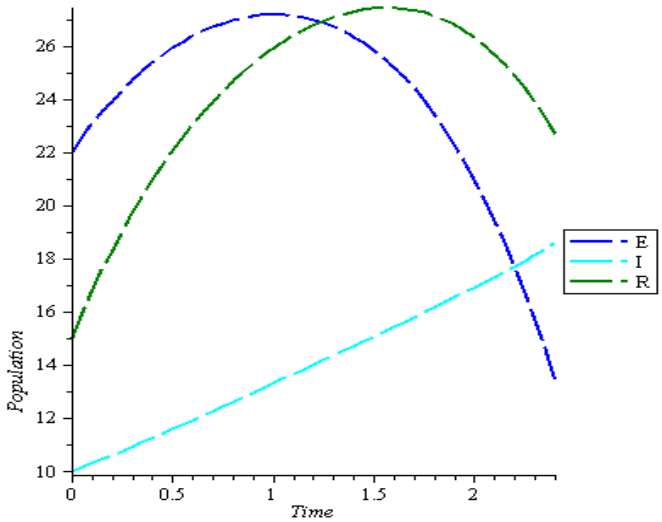

Figure 6 Influence of vaccination rate on the E_I_R at $\rho = 0.6$.

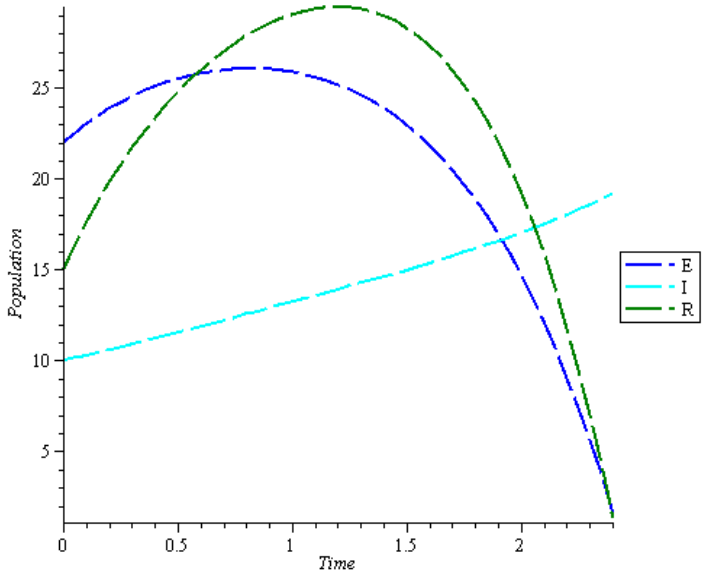

Figure 7 Influence of vaccination rate on the E_I_R at $\rho = 0.9$.

As seen in **Figure 1**, if vaccination is implemented in the compartments at a rate which progresses from 0 to 0.9, more people tend to be susceptible to the disease and fewer people will get exposed. Likewise in the exposed class, the increment in vaccination rate was studied and as seen in **Figure 2**, the rate of the inhabitants which are exposed reduces drastically as vaccination rate increases. Since proper and quality vaccination against infectious diseases leads to recovery of patients from it sting, **Figure 3** reveal the influence of high vaccination rate in the recovered class. As seen from the graph, more people tend to get recovered in the class as there is increment in vaccination. **Figures 4** - **7** shows the overall impact of vaccination in the 3 classes (Exposed, Infected and Recovered) considered. As seen from the figures, the exposed and recovered inhabitants' increases as the rate by which vaccination are implemented increases.

Conclusions

In this work, a mathematical model of COVID-19 incorporated with media-induced fear and vaccination was analysed and simulated. We are able to deduce analytically that the stability of the system basically depends on the Basic reproduction number R_0. In **Figures 1** - **3** the effect of vaccination on the susceptible, exposed and recovered class of the model was presented by simulation of the approximate results obtained numerically using the homotopy perturbation method. When there is no fear in the compartment, the inhabitants of the classes tend to get exposed and infected with the disease as there is constant contact between the members of each class of the medium. This can easily lead to increment in the disease transmission coefficient and thus leads to instability of the system. As an alternative measure to curb the spread of the disease for the system to remain stable, another strategy such as vaccination which increases the herd immunity of the inhabitants can be employed.

References

[1] OM Ogunlaran and SCO Noutchie. Mathematical model for an effective management of HIV infection. *BioMed Res. Int.* 2016; **2016**, 4217548.
[2] MO Olayiwola and MK Kolawole. Some results on the simulation of SEIRS epidemic model with saturated incidence rate for considering the saturation term for susceptible individual. *Ann. Comput. Sci. Ser.* 2017; **15**, 9-18.
[3] JH He. Homotopy perturbation technique. *Comput. Methods Appl. Mech. Eng.* 1999; **178**, 257-62.
[4] JH He. Variational iteration method - a kind of non-linear analytical technique. *Int. J. Non-linear Mech.* 1999; **34**, 699-708.

[5] MO Olayiwola, MK Kolawole and AO Popoola. Variational iteration method for the simulation of the effect of transmission coefficient on the susceptible-exposed-infected-recovered-susceptible (SEIRS) epidemic model with saturated incidence rate. *J. Sci. Arts* 2017; **17**, 357-64.
[6] MK Kolawole and MO Olayiwola. On the numerical simulation of the effect of saturation term on the susceptible individual in Susceptible-Exposed Infected-Recovered-Susceptible (SEIRS) epidemic model. *Comput. Inf. Syst. Dev. Inf. Allied Res. J.* 2016; **7**, 83.
[7] S Balamuralitharan and S Geethamalini. Solutions of epidemic of EIAV infection by HPM. *J. Phys.: Conf. Ser*. 2018; **1000**, 12023.
[8] M Farman, MU Saleem, A Ahmad and MO Ahmad. Analysis and numerical simulation of SEIR epidemic model of measles with a non-integer time fractional derivative using the Laplace Adomian decomposition method. *Ain Shams Eng. J.* 2018; **9**, 3391-7.
[9] H Fazal, S Kamal, R Ghausur and S Muhammad. Numerical solution of fractional order smoking model via laplace Adomian decomposition method. *Alex. Eng. J.* 2018; **57**, 1061-9.
[10] G Adomian. A review of the decomposition method and some recent results for nonlinear equations. *Comput. Math. Appl.* 1991; **21**, 101-27.
[11] C Maji. Impact of media induced fear on the control on covid-19 outbreak: A mathematical study. *Int. J. Differ. Equ*. 2021; **2021**, 2129490.
[12] B Ivorra and AM Ramos. Application of the Be-CoDis mathematical model to forecast the international spread of the 2019-20 Wuhan coronavirus outbreak. *Complutense Univ. Madrid* 2020. http://dx.doi.org/10.13140/RG.2.2.31460.94081
[13] JKK Asamoah, Z Jin, GQ Sun, B Seidu, E Yankson, A Abidemi, FT Oduro, SE Moore and E Okyere. Sensitivity assessment and optimal economic evaluation of a new COVID-19 compartmental epidemic model with control interventions. *Chaos Solitons Fractals* 2021; **146**, 110885.
[14] JKK Asamoah, MA Owusu, Z Jin, FT Oduro, A Abidemi and EO Gyasi. Global stability and cost-effectiveness analysis of COVID-19 considering the impact of the environment: Using data from Ghana. *Chaos Solitons Fractals* 2020; **140**, 110103.
[15] KA Bashiru, AO Fasoranbaku, O Adebimpe and TA Ojurongbe. Stability analysis of Mother - to - Child Transmission of HIV/AIDS Dynamic Model with Treatment. *Annal. Comput. Sci. Series J.* 2017; **15**, 89-93.
[16] MS Abdo, K Shah, HA Wahash and SK Pancha. On a comprehensive model of the novel coronavirus (COVID-19) under Mittag-Leffler derivative. *Chaos Solutions Fractals* 2020; **135**, 109867.
[17] MAA Al-Qaness, AA Ewees, H Fan, A Aziz and MAE Aziz. Optimization method for forecasting confirmed cases of COVID-19 in China. *J. Clin. Med*. 2020; **9**, 674.
[18] Worldometer, Available at: https://www.worldometers.info, accessed March 2022.
[19] World Population Review, Available at: https://worldpopulationreview.com, accessed March 2022.